Supplementary Information

Simultaneous detection of SARS-CoV-2 RNA and host antibodies enabled by a multiplexed electrochemical sensor platform

Helena de Puig[1, 2 #], Sanjay Sharma Timilsina[1 #], Joshua Rainbow[1, 3 #], Pawan Jolly[1 #], Devora Najjar[1, 2, 4], Nolan Durr[1], Galit Alter[5], Jonathan Z. Li[6], Xu G. Yu[5, 6], David R. Walt[1, 7, 8], Pedro Estrela[3], James J. Collins[1, 2, 9], Donald E. Ingber[1, 7, 10, 11 *]

[1]Wyss Institute for Biologically Inspired Engineering, Harvard University, Boston, MA 02115, USA
[2]Institute for Medical Engineering and Science, Department of Biological Engineering, Massachusetts Institute of Technology, Cambridge, MA 02139, USA
[3]Centre for Biosensors, Bioelectronics and Biodevices (C3Bio) and Department of Electronic and Electrical Engineering, University of Bath, Bath BA2 7AY, UK
[4]MIT Media Lab, Massachusetts Institute of Technology, Cambridge, MA 02139, USA
[5]Ragon Institute of MGH, MIT, and Harvard, Cambridge, MA 02139, USA.
[6]Division of Infectious Diseases, Brigham and Women's Hospital, Boston, MA 02115, USA
[7]Harvard Medical School, Boston, MA 02115, USA
[8]Department of Pathology, Brigham and Women's Hospital, Boston, MA 02115, USA
[9]Infectious Disease and Microbiome Program, Broad Institute of MIT and Harvard, Cambridge, MA 02142, USA
[10]Vascular Biology Program and Department of Surgery, Boston Children's Hospital, Boston, MA 02115, USA
[11]Harvard John A. Paulson School of Engineering and Applied Sciences, Harvard University, Boston, MA 02115, USA

* Address all correspondence to: Donald E. Ingber, MD, PhD, Wyss Institute at Harvard University, CLSB5, 3 Blackfan Circle, Boston MA 02115, USA (phone: 617-432-7044, fax: 617-432-7828; e-mail: don.ingber@wyss.harvard.edu
# These authors contributed equally

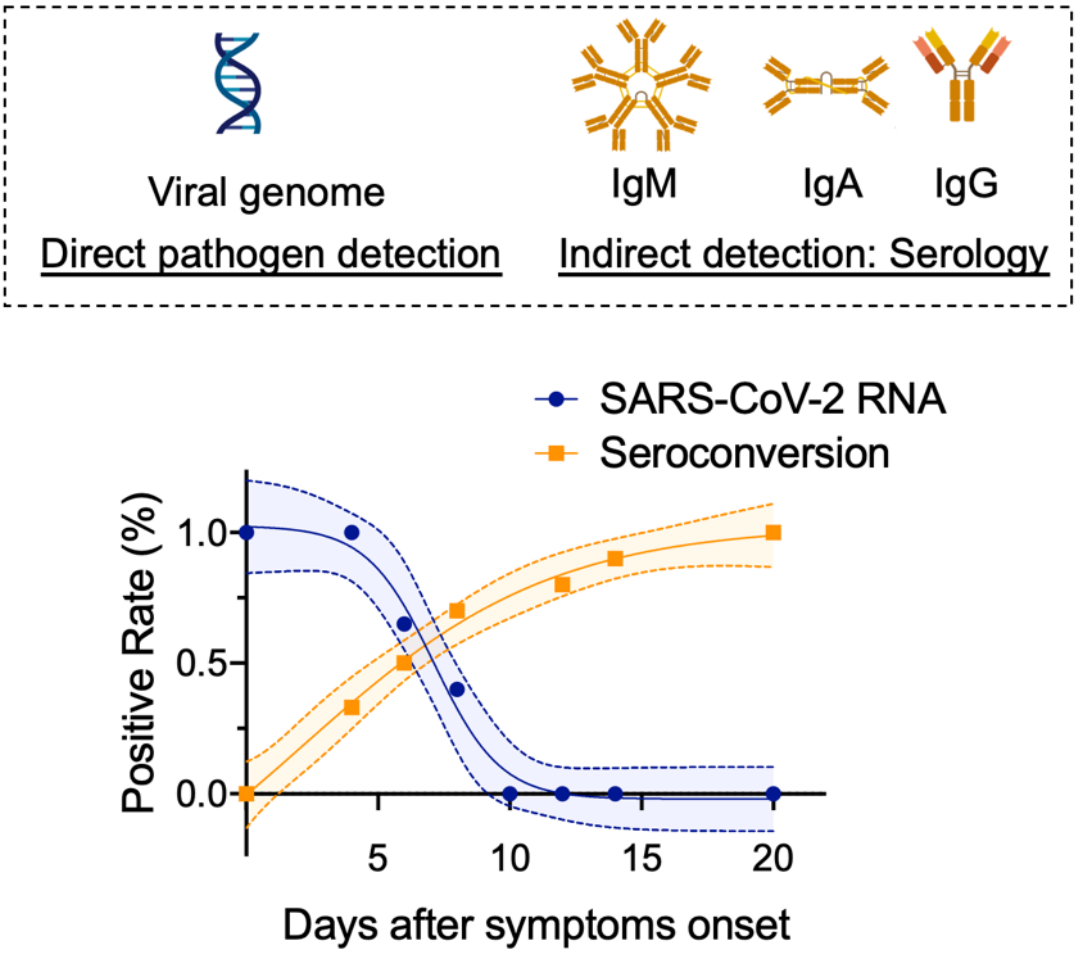

Fig. S1: Pathogen detection approaches: Direct pathogen detection approaches detect the virus, its genome or viral antigens. These assays are useful during the acute phase of disease, typically 0-7 days after symptoms. Serology assays measure the presence of host antibodies, such as IgG, IgM or IgA, that the patient generates during adaptive immune response to the disease. Data replotted from [1,62].

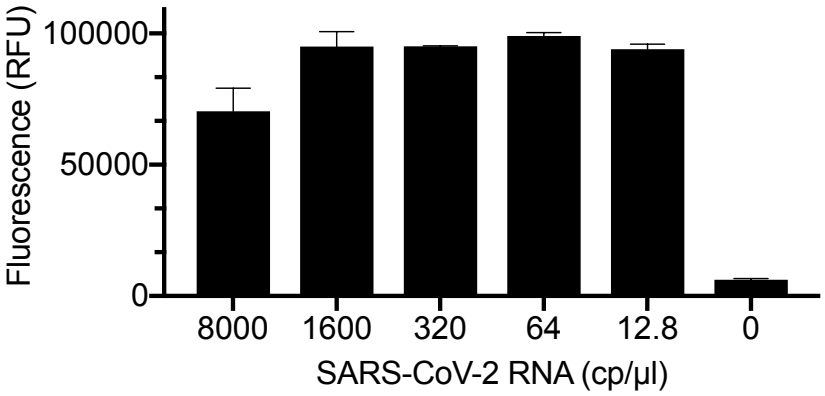

Figure S2: Limit of detection of the CRISPR-based assay with a fluorescence output. Serially diluted full-length SARS-CoV-2 RNA was spiked in water and amplified by RT-LAMP. Results show that dilutions down to 12.8 cp/μL of viral RNA had a clear positive signal (Student's t test p value <0.001) in our fluorescence-based assays. Error bars represent the standard deviation of triplicate experiments, biological replicates.

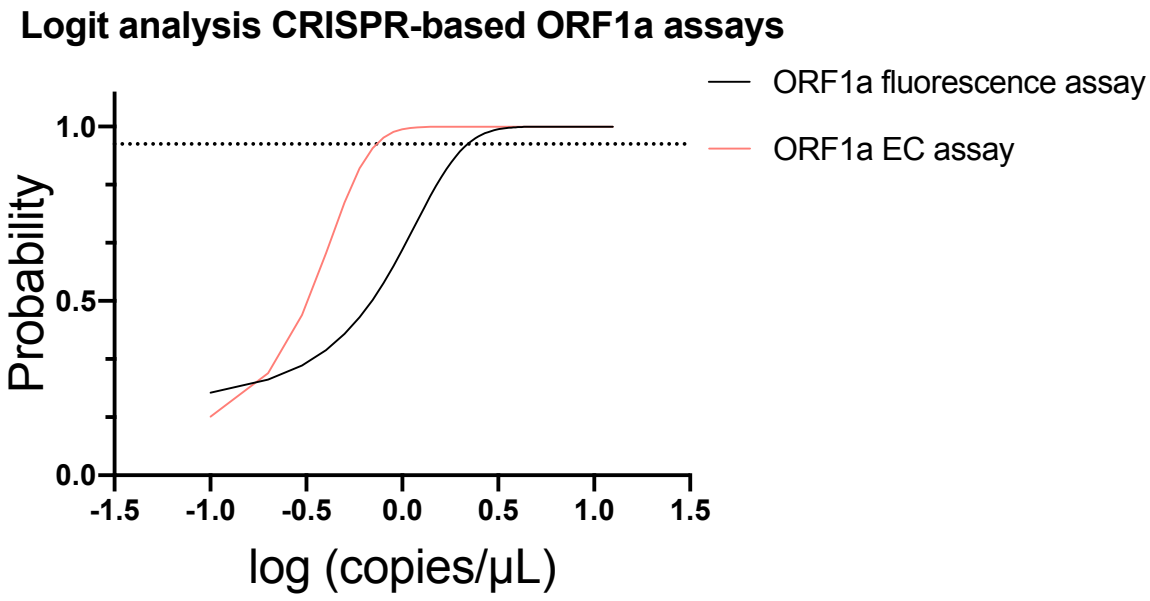

Figure S3: Sensitivity of the viral RNA electrochemical assay was higher than the fluorescence output by comparing logit regression curves and their fit characteristics. Serially diluted full-length SARS-CoV-2 RNA was spiked in water and amplified by RT-LAMP. Results show that dilutions down to 0.8 cp/μL of viral RNA had 95% probability of leading to a clear positive signal in our electrochemical platform (red). In contrast, the limit of detection in the fluorescence-based platform was 2.3cp/μl (black). The supplementary table S1 contains the raw data used to fit the logit function. Each concentration was probed with 5 independent biological replicates.

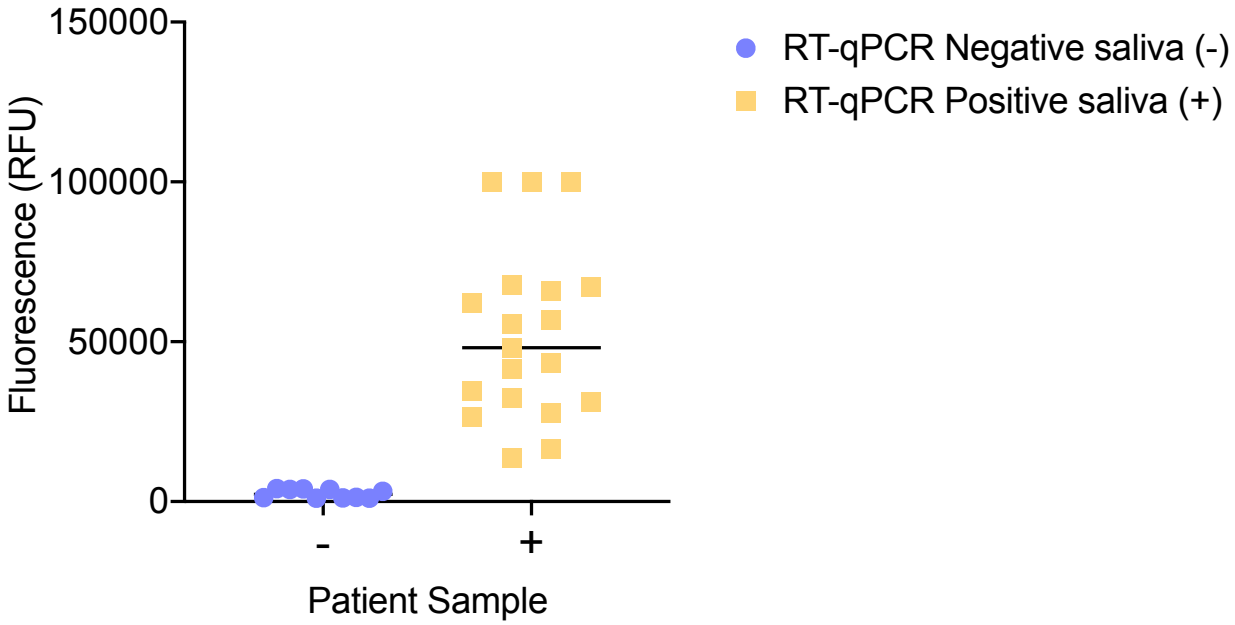

Figure S4: CRISPR-based fluorescence assays can diagnose SARS-CoV-2 positive and negative clinical samples. SARS-CoV-2 RT-qPCR positive saliva (+, orange) shows a high fluorescence signal whereas negative samples (-, blue) show a low fluorescence signal. Unpaired Student's t test $p<0.0001$ for differences in fluorescence between SARS-CoV-2 positive and negative samples.

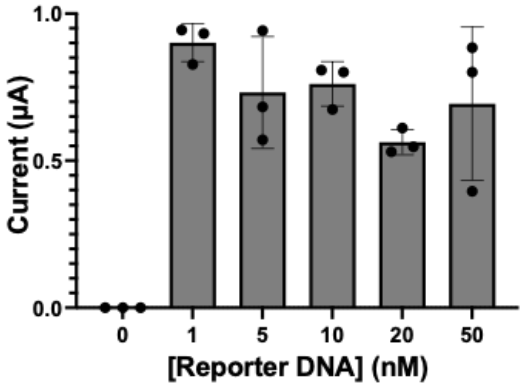

Figure S5: Optimization of the reporter concentrations in the CRISPR-electrochemistry RNA assay. We optimized the concentration of the biotinylated reporter probe for the electrochemical SARS-CoV-2 CRISPR-based RNA assays. We tested reporter concentrations between 0-50 nM and obtained optimal performance of the assays at 1nM final reporter concentration. Error bars represent the standard deviation of biological triplicate experiments.

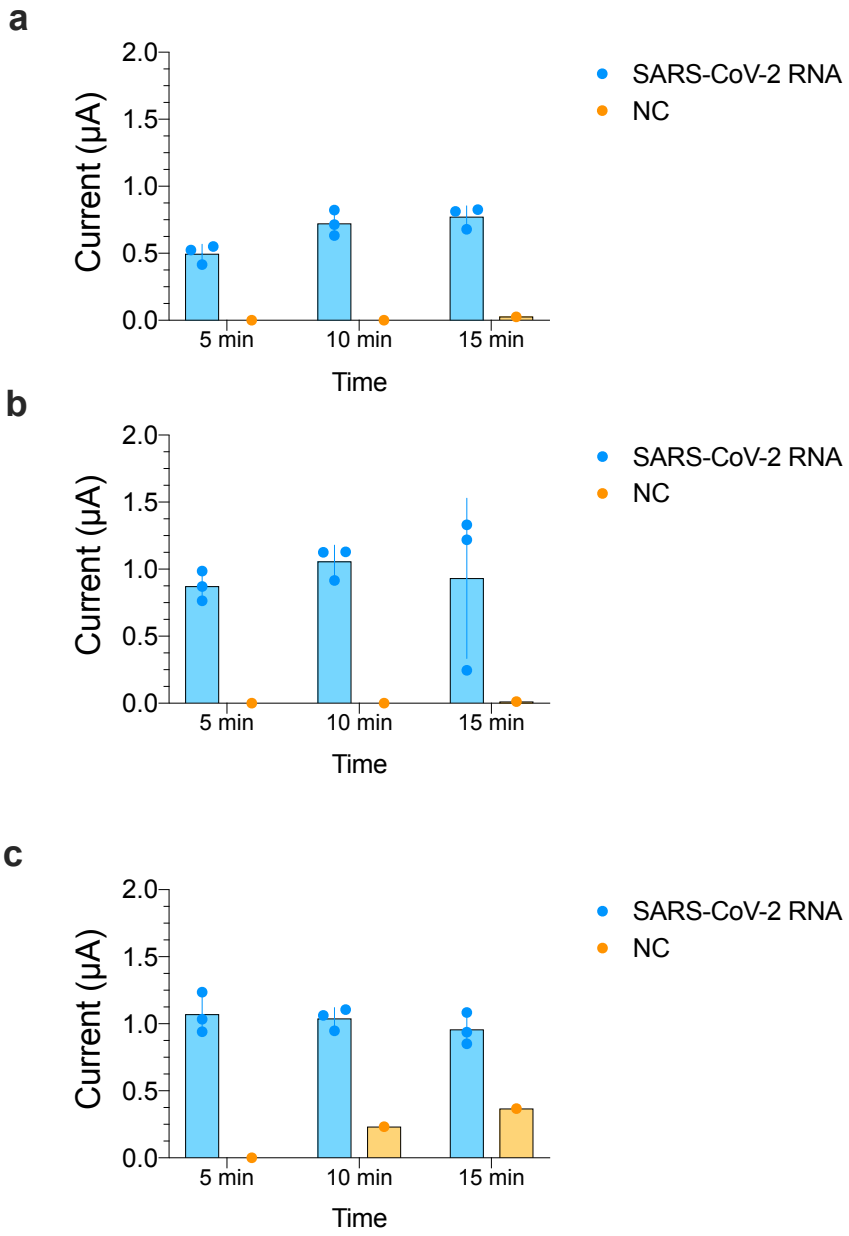

Figure S6: Optimization of the CRISPR-electrochemistry assay time. We optimized the reaction times by incubating (a) 0.5nM, (b) 1nM and (c) 5nM reporter probes over 5, 10 and 15 min. We selected 1nM reporter probe concentration and 5 min incubation times for further experiments. Error bars represent standard deviation of biological independent triplicate experiments.

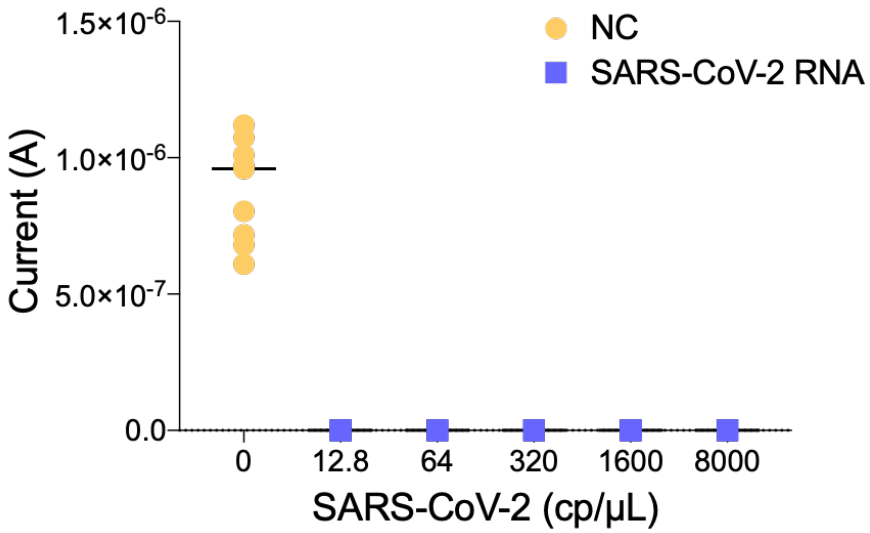

Figure S7: Limit of detection of the CRISPR-based electrochemical assay. Serially diluted full-length SARS-CoV-2 RNA was spiked in water and amplified by RT-LAMP. Results show that dilutions down to 12.8 cp/μL of viral RNA had a clear negative signal in our electrochemical assays, indicating no deposition of TMB. Unpaired Student's t-test $p<0.0001$ for differences in current (A) between 12.8 cp/μl and 0 cp/μl viral RNA. NC: negative control, 0cp/μl viral RNA. Error bars represent the standard deviation of independent triplicate experiments, biological replicates.

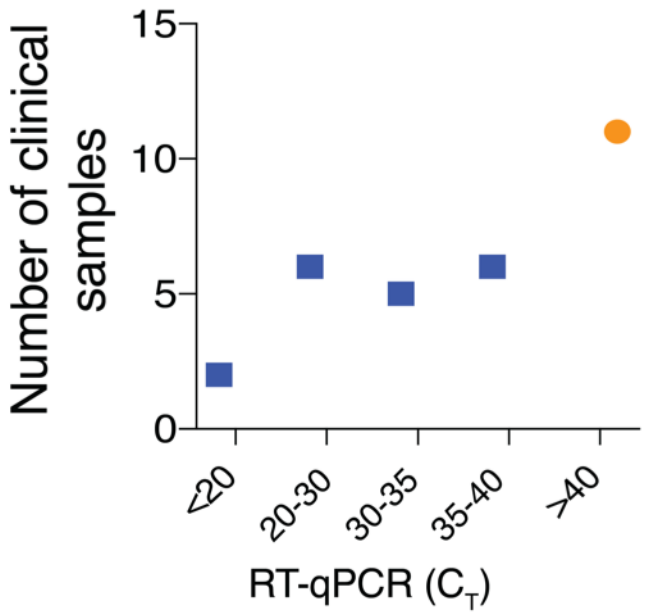

Figure S8: Clinical SARS-CoV-2 saliva samples with a wide range of RT-qPCR cycle threshold (C_T) plotted against the number of samples tested in our device.

a

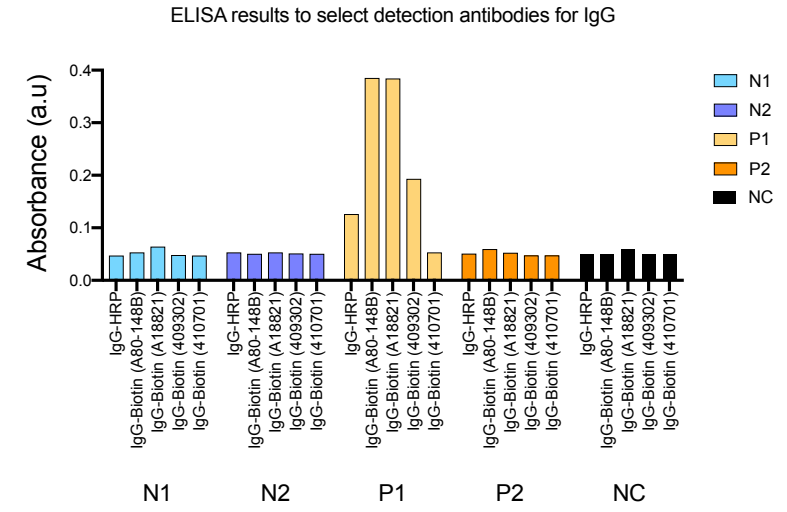

Different IgG detection antibodies tested against two SARS-Cov-2 Positive (P) and Negative (N) Samples

b

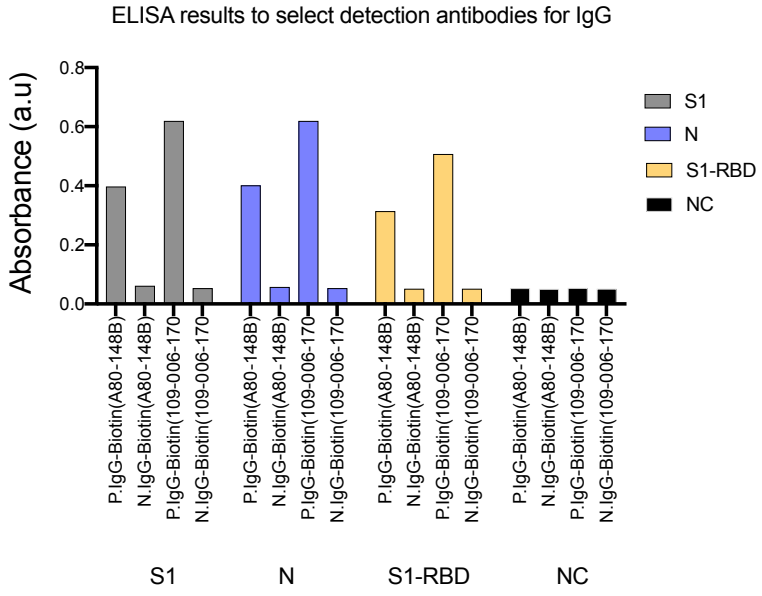

Two IgG detection antibodies tested against all three antigens (S1, N and S1-RBD) and two SARS-Cov-2 Positive (P) and Negative (N) Samples

Figure S9: Selection of the SARS-CoV-2 anti-human IgG detection antibody against Spike, NC, and RBD protein in an ELISA format using SARS-CoV-2 positive and negative samples. (a) Biotinylated goat anti-human IgG Biotin (A80-148B) and (A18821) had high signals for positive sample P1. All detection antibodies gave a similar low signal for negative clinical samples and PBS negative control background (Supplementary Fig. S12a). Overall, the anti-IgG Biotin (A80-148B) had a higher signal-to-noise ratio. (b) Comparison of the performance of anti-IgG Biotin (A80-148B) with anti-IgG Biotin (109-006-170) using antigens S1, N, and S1-RBD. Anti-IgG Biotin (109-006-170) was selected for further experiments because it had higher signal-to-noise ratios for all antigens.

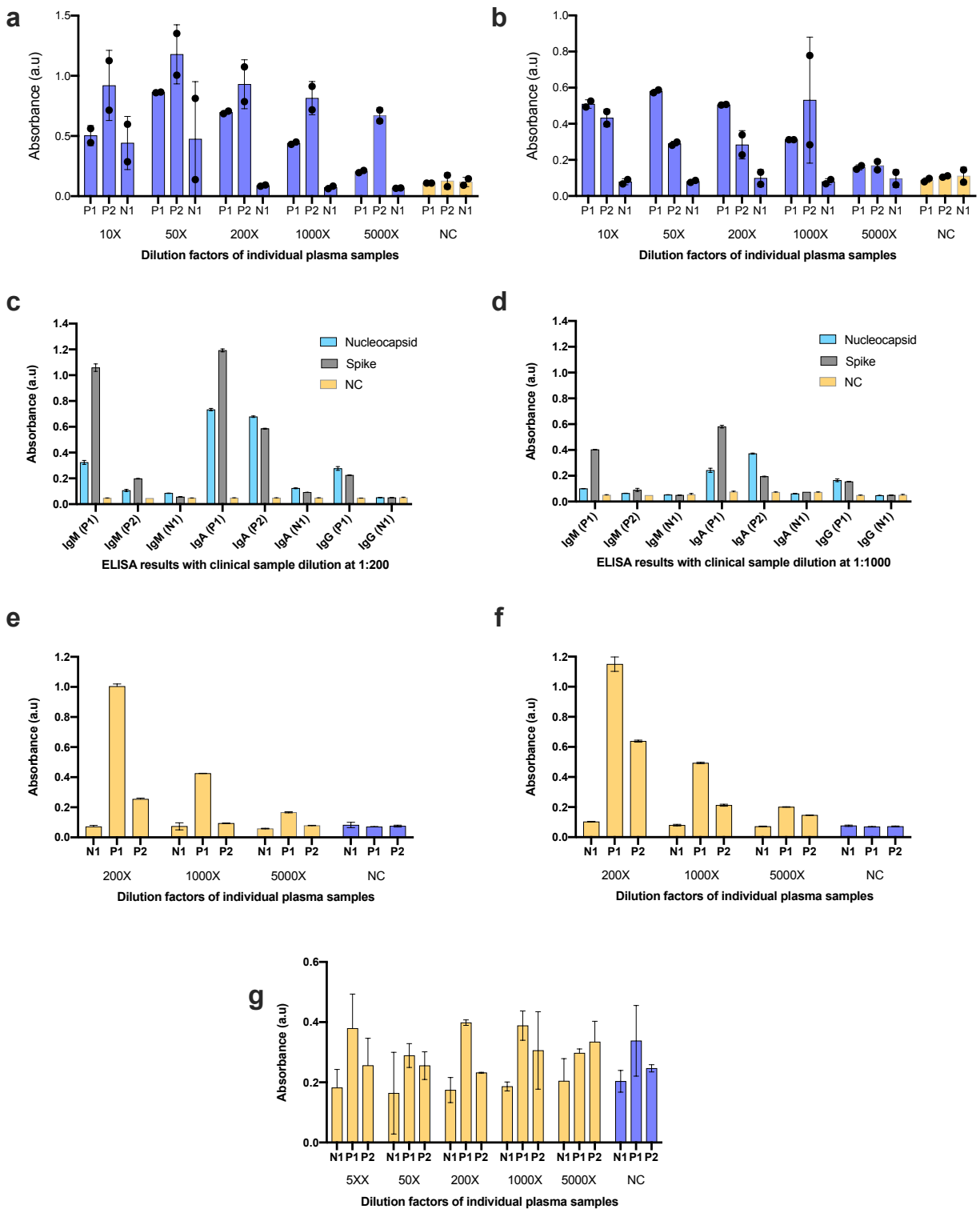

Figure S10: Optimization of the plasma dilutions using clinical plasma samples in a 96-well ELISA format. Serial plasma dilutions were tested in an ELISA plate format with immobilized antigens (a) nucleocapsid and (b) spike protein. Plasma diluted at (c) 200-fold and (d) 1000-fold were compared in ELISA plate formats to detect human IgM, IgA and IgG antibodies against

immobilized nucleocapsid and Spike protein. Serial plasma dilutions were tested in an ELISA plate format with immobilized S1-RBD to detect human (e) IgM, (f) IgA and (g) IgG. We observe that dilutions between 200X-1000X show a high signal-to-noise ratio in ELISA when detecting IgG against both N and S1 protein antigens (a) and (b), respectively. The dilution factor of 200X (c) detected the less abundant antibody isotypes (IgM and IgA). Similar results were obtained when immobilizing the S1-RBD antigen (e-g), indicating that a dilution factor of 200X was optimal for ELISA experiments. Error bars represent the standard deviation of independent triplicate experiments, biological replicates.

A

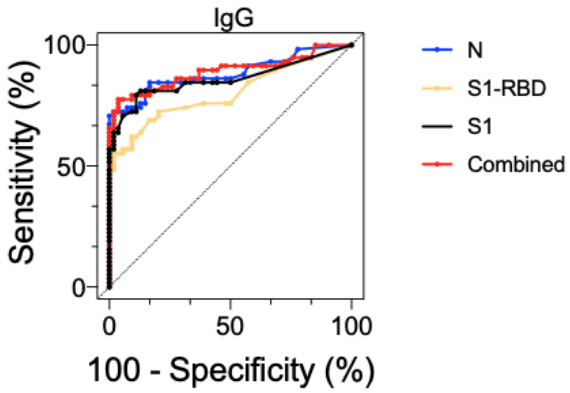

B

	IgG			
	S1	S1-RBD	N	Combined
AUC	0.86	0.80	0.88	0.89
95% conf. int.	[0.78-0.93]	[0.72-0.88]	[0.82-0.95]	[0.82-0.96]
P value	<0.0001	<0.0001	<0.0001	<0.0001
Cutoff	>0.018	>0.022	>0.041	>0.064
Sens.	0.64 [0.51-0.75]	0.57 [0.44-0.69]	0.72 [0.60-0.82]	0.72 [0.60-0.82]
Spec.	0.98 [0.90-1.00]	0.94 [0.85-0.99]	0.98 [0.90-1.00]	0.98 [0.90-1.00]
N pos.	54	54	54	54
N neg.	58	58	58	58

Figure S11: ELISA assays detect SARS-CoV-2-specific IgG antibodies in plasma samples. (a) Receiver operating characteristic (ROC) curve analysis of the patient sample data collected for the IgG SARS CoV-2 assay using results from 54 prior- RT-qPCR confirmed positive and 58 negative human plasma samples. (b) Table listing numerical values of the ROC curve analysis. AUC: area under the curve; 95% conf. Int.: 95% confidence interval; Sens: sensitivity; Spec.: specificity; N pos.: number of RT-qPCR SARS-CoV-2 positive samples; N neg.: number of RT-qPCR SARS-CoV-2 negative clinical samples.

A

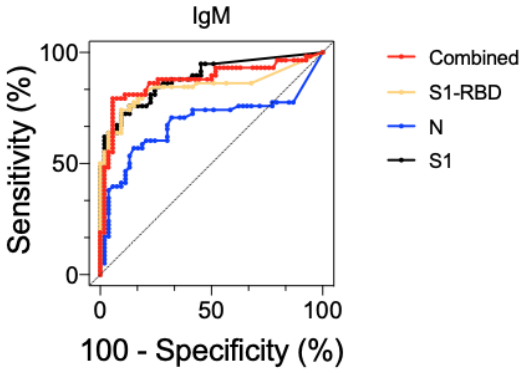

B

	IgM			
	S1	S1-RBD	N	Combined
AUC	0.89	0.84	0.68	0.87
95% conf. int.	[0.82-0.95]	[0.77-0.92]	[0.58-0.79]	[0.80-0.95]
P value	<0.0001	<0.0001	0.0009	<0.0001
Cutoff	>0.007	>0.067	>0.080	>0.128
Sens.	0.62 [0.49-0.73]	0.55 [0.42-0.67]	0.38 [0.27-0.51]	0.79 [0.67-0.88]
Spec.	0.98 [0.90-1.00]	0.98 [0.90-1.00]	0.96 [0.87-0.99]	0.94 [0.85-0.99]
N pos.	54	54	54	54
N neg.	58	58	58	58

Figure S12: ELISA assays can detect SARS-CoV-2-specific IgM antibodies in plasma samples. (a) Receiver operating characteristic (ROC) curve analysis of the patient sample data collected for the IgM SARS CoV-2 assay using results from 54 prior- RT-qPCR confirmed positive and 58 negative human plasma samples. (b) Table listing numerical values of the ROC curve analysis. AUC: area under the curve; 95% conf. Int.: 95% confidence interval; Sens: sensitivity; Spec.: specificity; N pos.: number of RT-qPCR SARS-CoV-2 positive samples; N neg.: number of RT-qPCR SARS-CoV-2 negative clinical samples.

A

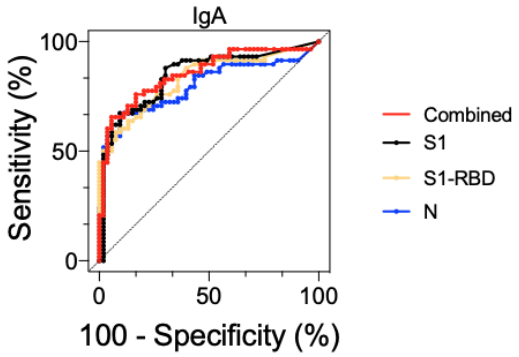

B

	IgA			
	S1	S1-RBD	N	Combined
AUC	0.85	0.83	0.80	0.85
95% conf. int.	[0.77-0.92]	[0.75-0.91]	[0.71-0.88]	[0.78-0.93]
P value	<0.0001	<0.0001	<0.0001	<0.0001
Cutoff	>0.110	>0.115	>0.260	>0.376
Sens.	0.48 [0.36-0.61]	0.50 [0.38-0.63]	0.52 [0.39-0.64]	0.60 [0.48-0.72]
Spec.	0.98 [0.90-1.00]	0.98 [0.90-1.00]	0.98 [0.90-1.00]	0.96 [0.88-0.99]
N pos.	54	54	54	54
N neg.	58	58	58	58

Figure S13: ELISA assays can detect SARS-CoV-2-specific IgA antibodies in plasma samples. (a) Receiver operating characteristic (ROC) curve analysis of the patient sample data collected for the IgA SARS CoV-2 assay using results from 54 prior- RT-qPCR confirmed positive and 58 negative human plasma samples. (b) Table listing numerical values of the ROC curve analysis. AUC: area under the curve; 95% conf. Int.: 95% confidence interval; Sens: sensitivity; Spec.: specificity; N pos.: number of RT-qPCR SARS-CoV-2 positive samples; N neg.: number of RT-qPCR SARS-CoV-2 negative clinical samples.

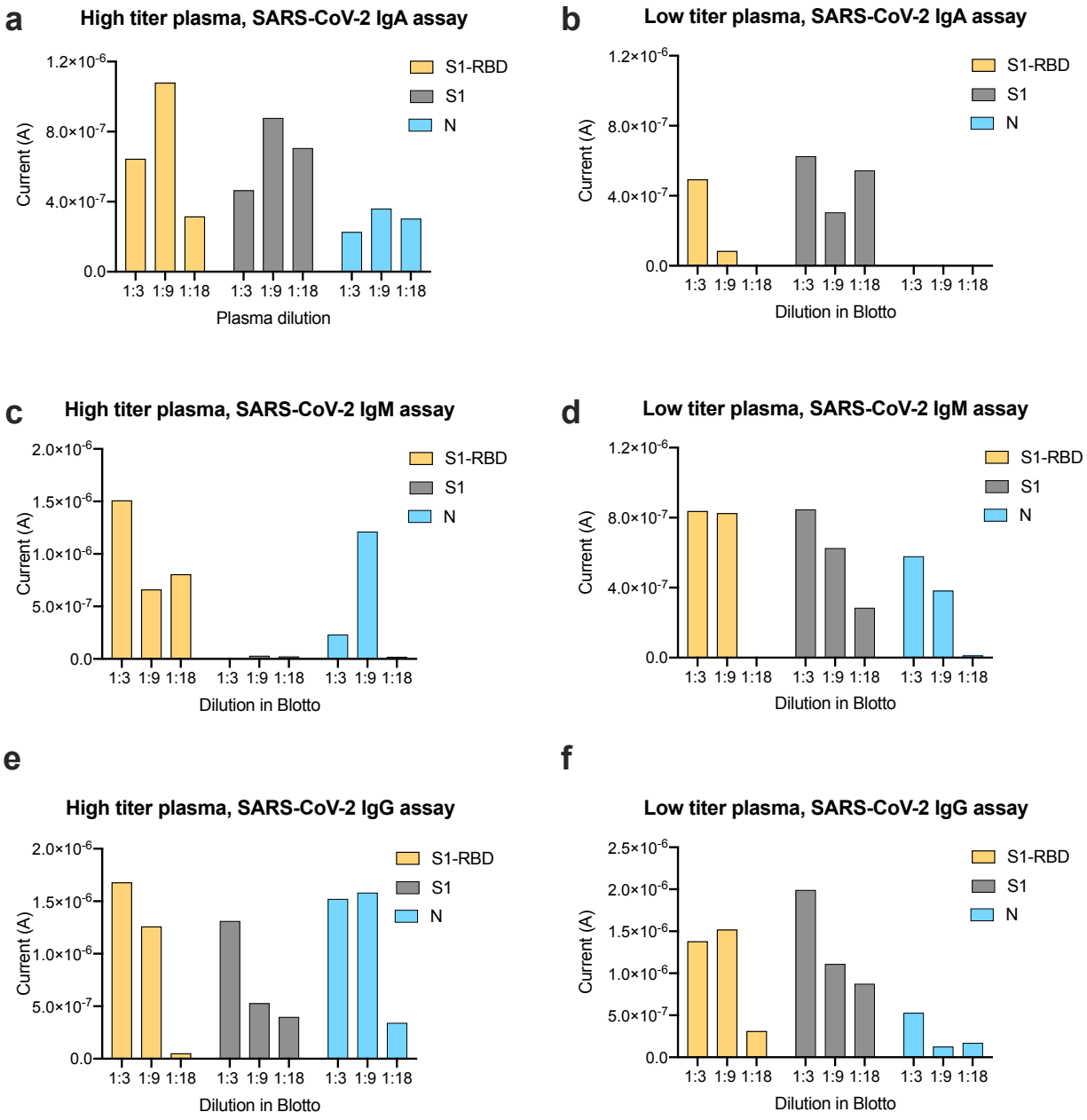

Figure S14: A sample dilution of 1:9 is optimal for IgG, IgM and IgA detection in the electrochemical platform. High and low antibody titer plasma was serially diluted and tested on the electrochemical platform to detect anti-SARS-CoV-2 human (a, b) IgA, (c, d) IgM, and (e, f) IgG against S1, nucleocapsid, and S1-RBD antigens immobilized on the electrodes.

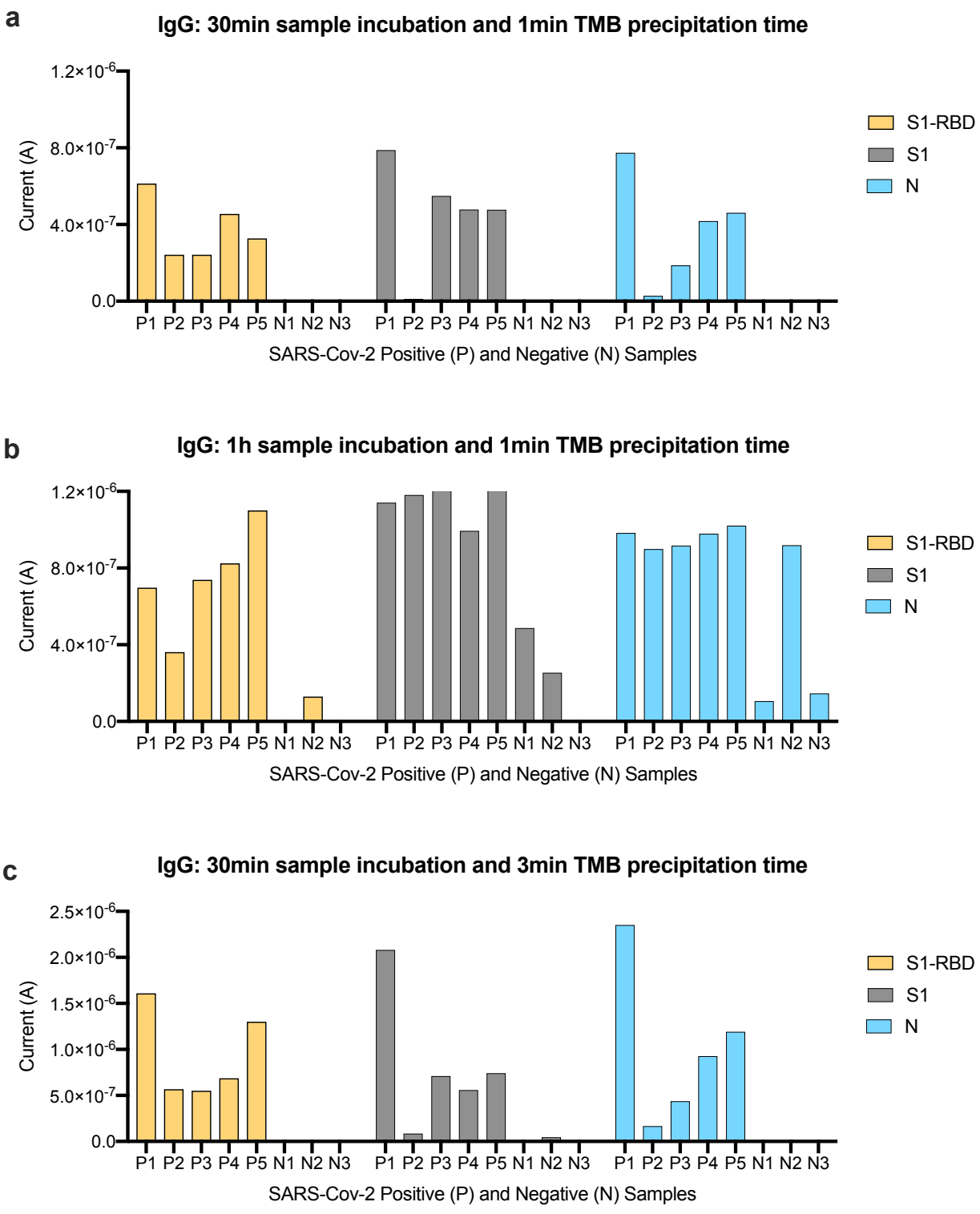

Figure S15: Optimization of the incubation and TMB precipitation times in 1:9 plasma dilutions. Electrochemical-biosensors were conjugated with the three antigens (S1-RBD, S1 and N) and used to detect IgG in a subset of positive and negative clinical plasma samples diluted at 1:9. We optimized the incubation and TMB precipitation times: (a) diluted plasma was incubated for 30

min and TMB was allowed to precipitate for 1 min (b) diluted plasma was incubated for 1h and TMB precipitation time was 1 min; (c) diluted plasma was incubated for 30 min and TMB reactions proceeded for 3 min. We observed that the optimal performance was obtained for (c) 3 min plasma incubation on the electrodes and 3min TMB precipitation.

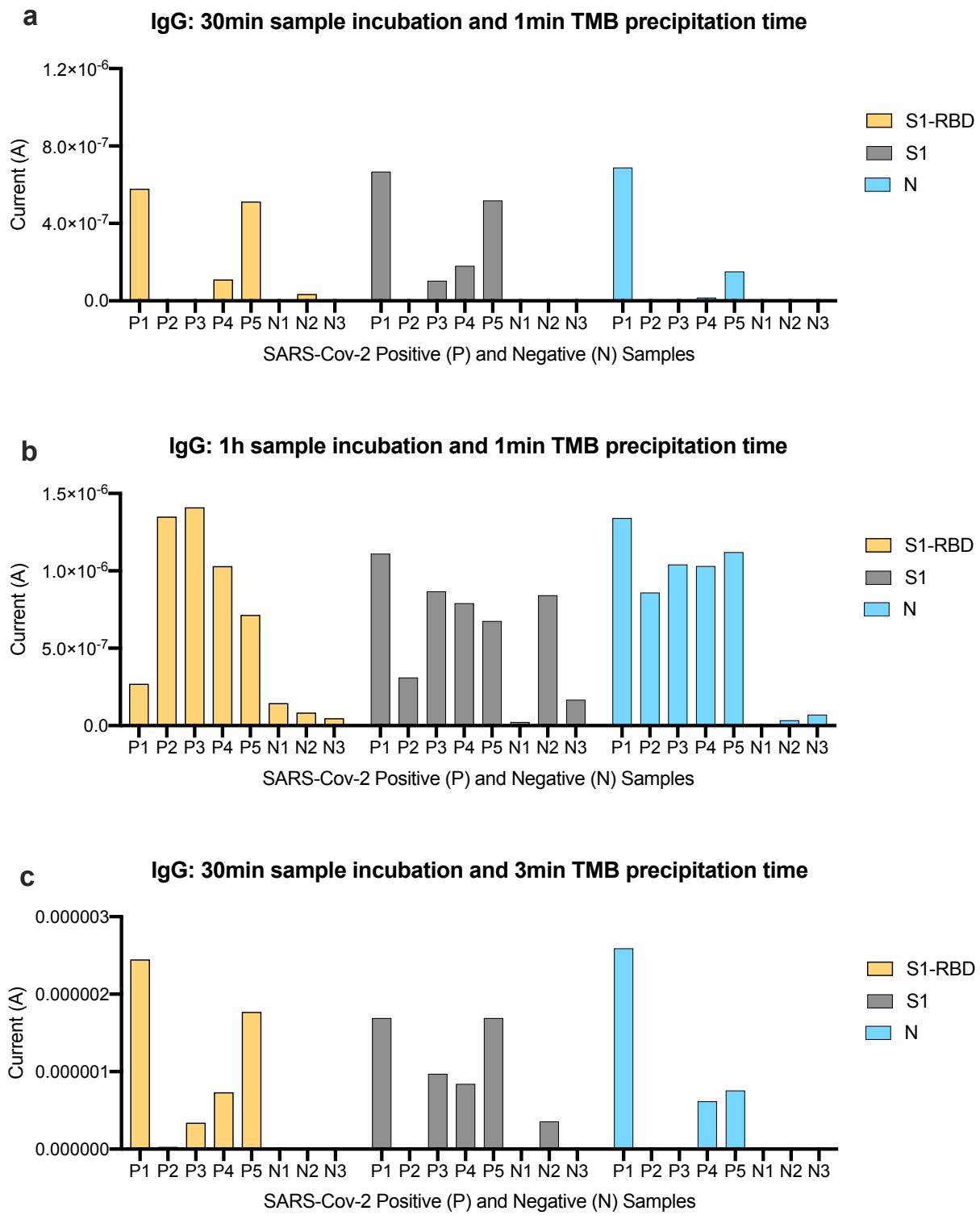

Figure S16: Optimization of incubation and TMB precipitation time at 1:18 plasma dilutions. Electrochemical-Biosensors were conjugated with the three antigens (S1-RBD, S1 and N), and used to detect IgG in a subset of positive and negative clinical plasma samples diluted at 1:18. We optimized the incubation and TMB precipitation times: (a) diluted plasma samples were incubated for

30 min and TMB was allowed to precipitate for 1 min (b) diluted plasma samples were incubated for 1h and TMB precipitation time was 1 min; (c) diluted plasma samples were incubated for 30 min and TMB reactions proceeded for 3 min. Optimal performance was observed for plasma diluted at 1:9 (Supplementary Figure S15c).

A

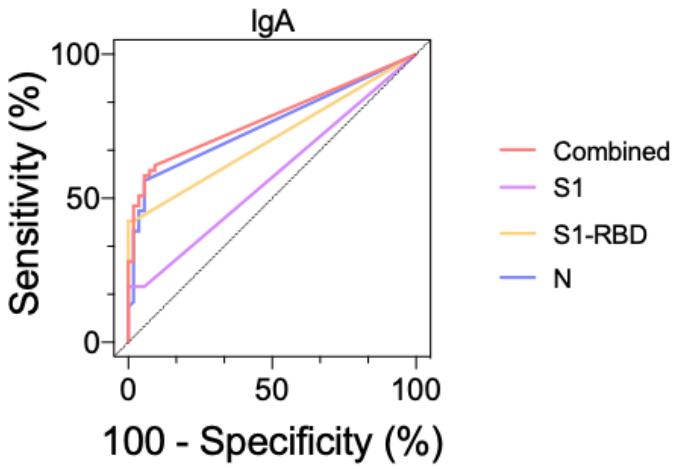

B

	IgA			
	S1	S1-RBD	N	Combined
AUC	0.57	0.76	0.71	0.78
95% conf. int.	[0.47-0.68]	[0.66-0.85]	[0.61-0.80]	[0.69-0.87]
P value	0.18	<0.0001	0.0002	<0.0001
Cutoff	>4.14e-8	>4.1e-7	>5.3e-8	>4.5e-8
Sens.	0.19 [0.11-0.31]	0.39 [0.27-0.52]	0.42 [0.30-0.55]	0.58 [0.45-0.70]
Spec.	1 [0.27-0.52]	0.98 [0.90-1.00]	1 [0.93-1.00]	0.94 [0.85-0.99]
N pos.	54	54	54	54
N neg.	58	58	58	58

Figure S17: Electrochemical serological assays can detect SARS-CoV-2-specific IgA antibodies in plasma samples. (a) Receiver operating characteristic (ROC) curve analysis of the patient sample data collected for the IgA SARS CoV-2 electrochemical assay using results from 54 prior- RT-qPCR confirmed positive and 58 negative human plasma samples. (b) Table listing numerical values of the ROC curve analysis. AUC: area under the curve; 95% conf. Int.: 95% confidence interval; Sens: sensitivity; Spec.: specificity; N pos.: number of RT-qPCR SARS-CoV-2 positive samples; N neg.: number of RT-qPCR SARS-CoV-2 negative clinical samples.

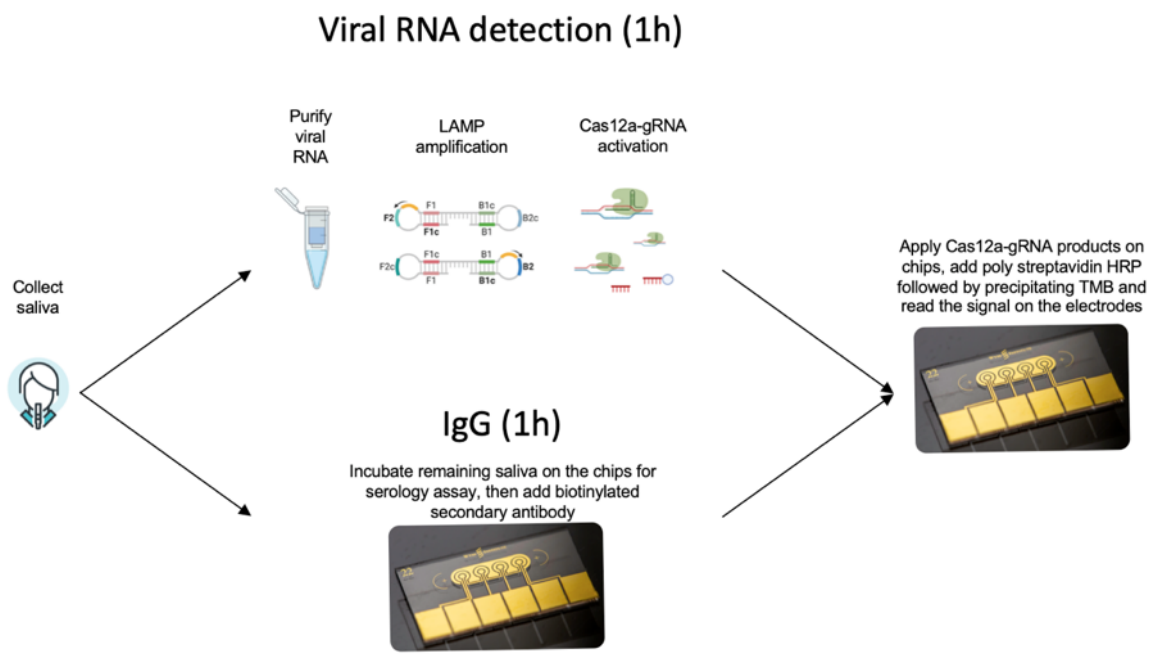

Figure S18: Schematic workflow of the multiplexed electrochemical sensor platform for the simultaneous detection of SARS-CoV-2 RNA and host antibodies. Multiplexed electrochemical chips were conjugated with antigens S1, S1-RBD and N, as well as the PNA reporter. SARS-CoV-2 positive and negative saliva were heat-inactivated, spiked with human plasma at 1:20 and separated into two groups: (1) 20μl of the IgG-spiked saliva were incubated on the electrodes followed by incubation with biotinylated anti-human IgG. (2) The remaining saliva went through RNA extraction, followed by LAMP and CRISPR-Cas RNA detection with the EC biotinylated probe, and further incubated on the electrodes. Finally, the sensors were incubated with poly streptavidin-HRP and precipitating TMB, followed by electrochemical readout.

								LOD (cp/μl)
Fluorescent assay	RNA (cp/μl)	12.5	6.25	1	0.3	0.15	0	2.3
	Replicates (+/total)	5/5	5/5	3/5	2/5	2/5	0/5	
Electrochemical assay	RNA (cp/ μl)	12.5	6.25	1	0.3	0.15	0	0.8
	Replicates (+/total)	5/5	5/5	5/5	3/5	2/5	0/5	

Supplementary Table S1: Raw data used for the logit regression curve analysis to measure the limit of detection of fluorescent and electrochemical CRISPR-based SARS-CoV-2 RNA detection.

	CRISPR fluorescence
AUC	1.00
95% conf. int.	[1.00-1.00]
P value	<0.0001
Cutoff	8859
Sens.	1.00 [0.83-1.00]
Spec.	1.00 [0.72-1.00]
N pos.	19
N neg.	10

Supplementary Table S2: CRISPR-based fluorescent assays accurately detect SARS-CoV-2 in clinical saliva samples. Numerical values of the Receiver operating characteristic (ROC) curve analysis of the patient sample data collected for the SARS CoV-2 assay using results from 19 RT-qPCR confirmed positive and 10 negative human saliva samples. AUC: area under the curve; 95% conf. Int.: 95% confidence interval; Sens: sensitivity; Spec.: specificity; N pos.: number of RT-qPCR SARS-CoV-2 positive samples; N neg.: number of RT-qPCR SARS-CoV-2 negative clinical samples.

Primer	Concentration	Sequence
FIP	1.6 µM	TCAGCACACAAAGCCAAAAATTTATTTTTCTGTG CAAAGGAAATTAAGGAG
BIP	1.6 µM	TATTGGTGGAGCTAAACTTAAAGCCTTTTCTGT ACAATCCCTTTGAGTG
F3	0.2 µM	CGGTGGACAAATTGTCAC
B3	0.2 µM	CTTCTCTGGATTTAACACACTT
LOOP F	0.4 µM	TTACAAGCTTAAAGAATGTCTGAACACT
LOOP B	0.4 µM	TTGAATTTAGGTGAAACATTTGTCACG

Supplementary Table S3: Best performing LAMP primer sequences and their final concentrations in LAMP assays[28].